Proc. of the 8th International Symposium on Geotechnical Safety and Risk (ISGSR)
Edited by Jinsong Huang, D.V. Griffiths, Shui-Hua Jiang, Anna Giacomini and Richard Kelly

doi: 10.3850/978-981-18-5182-7_20-007-cd

ISGSR 2022

Prediction of Punch-Through Risk of Spudcan Foundation Based on Bayesian Method

Yuan-Yuan Wang[1], Zhao-Feng Li[1], Wu-Zhang Luo[1] and Jin-Hui Li[1]

[1]School of Civil and Environmental Engineering, Harbin Institute of Technology, Shenzhen, China.
E-mail: jinhui.li@hit.edu.cn

Abstract: The installation of spudcan foundation of jack-up platforms in stiff-over-soft clay may occur punch-through failure due to the complexity of marine engineering geological conditions. However, the current deterministic methods recommended in the guidelines can only predict the peak penetration resistance of the spudcan foundation based on the assumption of uniform soils, which do not consider the uncertainty of soil properties in the complex seabed. Bayesian method can improve the predicted accuracy of peak penetration resistance and the corresponding depth by allowing the quantitative modeling of uncertainties in geometric and geotechnical parameters. This paper illustrates a developed Bayesian prediction model to realize the real-time prediction of peak penetration resistance and the corresponding depth. Different calculation models of peak penetration resistance and depth are applied to the Bayesian method to study the influence of different calculation models on the estimation of punch-though failure. The results show that the prediction accuracy increases with the increase of monitoring data, and the error of peak value by the developed Bayesian prediction model is within 5%.

Keywords: Spudcan foundation; Bearing capacity; Punch-through; Clays; Bayesian method.

1 Introduction

Mobile jack-up platforms are widely used for offshore drilling and gas industry in shallow to moderate water depths (up to ~120 m). A jack-up is installed by filling water ballast tanks on the platform, which pushes the legs and large inverted conical spudcan footings attached at the ends into the seabed soil. There is potential for a spudcan to punch through the strong clay into the underlying weak clay during installation, as shown in Figure 1. This punch-through failure can lead to buckling of the leg, effectively decommissioning the platform (Osborne & Paisley, 2002; Menzies & Lopez 2011; Jack *et al*., 2013; Hu *et al*., 2014). Two key parameters of punch-through failure are the peak penetration resistance and the depth of peak penetration resistance. If these parameters can be known before spudcan penetration, measures can be taken in advance to avoid punch-through accidents.

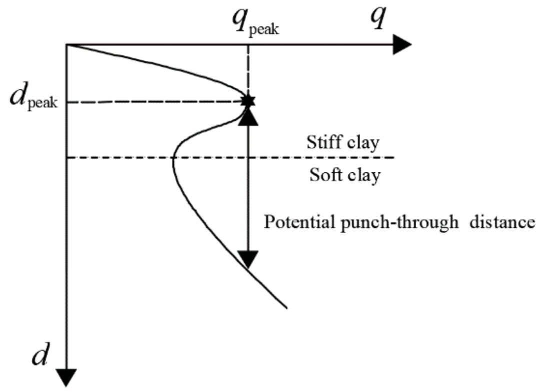

Figure 1. Illustration of potential punch-through

The deterministic method according to Brown and Meyerhof (1969) is recommended in the ISO (2016) and SNAME (2008). However, it doesn't give the punch-through criterion about the depth of peak penetration resistance and only applies to clay layers of uniform undrained shear strength. New deterministic methods are proposed to predict the depth of peak penetration resistance and suitable for nonhomogeneous strength profile (Hossain & Randolph, 2009; Zheng *et al*., 2016). Without accounting for the uncertainties, such as limited quantity of site investigations, variation in properties across a site and so on, the single-value prediction provided by the current deterministic methods is usually different from the field measurements (Van Dijk & Yetginer, 2015). Therefore, the probability method considering uncertainties has been proposed to predict the punch-through behavior of spudcan foundations. A model factor of calculation equation and probabilistic prediction model are proposed to define and characterize the uncertainties. The probability of the peak penetration resistance and the corresponding depth are continuously updated based on Bayesian theory during the penetration of spudcan foundations (Li *et al*., 2018; Marco *et al*., 2017). However, they only used a deterministic calculation model in the probability method for punch-through prediction. If other deterministic calculation model is used, can the probability method also get a good prediction? To answer this question, the semi-empirical model and the improved ISO model (Zheng *et al.*, 2016) are used in probabilistic prediction method to predict the punch-through failure of the spudcan foundation in this study, respectively.

2 Deterministic Model of Peak Resistance and Depth

A dataset of 57 geotechnical centrifuge model tests (Hossain & Randolph, 2010) and large deformation finite element (LDFE) analyses (Zheng *et al.*, 2016) form the basis of the deterministic model and of the probabilistic extension reported in this paper. The calculation model of the depth ($d_{\text{peak\_cal}}$) at which the peak penetration resistance occur, can be expressed as (Zheng *et al.*, 2016):

$$\frac{d_{\text{peak\_cal}}}{D} = 1.3\left(\frac{S_{\text{ubs}}}{S_{\text{ut}}}\right)^{1.5}\left(\frac{t}{D}\right)\left(1+\frac{kD}{S_{\text{ubs}}}\right)^{0.5} \le \frac{t}{D} \tag{1}$$

where D is the diameter of spudcan foundation; S_{ubs} is the intact undrained shear strength of bottom-layer soil at layer interface; S_{ut} is the intact undrained shear strength of top-layer soil; t is the thickness of the top-layer soil; and k is the rate of increase of shear strength within bottom layer.

The semi-empirical calculation model of peak penetration resistance, $q_{\text{peak\_semi}}$, can be expressed as (Zheng *et al.*, 2016):

$$\frac{q_{\text{peak\_semi}}}{S_{\text{ubs}}} = 6.35 + 5\left[\left(\frac{S_{\text{ubs}}}{S_{\text{ut}}}\right)^{-1}\left(\frac{t}{D}\right)^{0.75}\left(1+\frac{kD}{S_{\text{ubs}}}\right)^{0.5}\right]^{0.77} \tag{2}$$

The improved ISO calculation model of peak penetration resistance, $q_{\text{peak\_pro}}$, can be expressed as (Zheng *et al.*, 2016):

$$q_{\text{peak\_pro}} = \frac{4(t-d_{\text{peak\_cal}})}{D} \times 0.75 S_{\text{ut}} + \min\left[\left(6+1.2\frac{t}{D}\right), 9\right] S_{\text{ub}} + q_0 + 4.2\frac{T'}{D} S_{\text{ubs}} \tag{3}$$

where S_{ub} is the intact undrained shear strength of bottom-layer soil; q_0 is the effective overburden pressure of soils; and T' is equivalent thickness of soil plug (top-layer soil) in bottom layer.

3 Probabilistic Prediction Model

3.1 Uncertainty characterization

Since the deterministic model does not consider the uncertainty in soil properties caused by limited exploration data and inherent variability, the peak penetration resistance and the corresponding depth calculated by Eqs. (1) to (3) cannot be completely equal to the field measurements. In order to bridge this gap, the model factor is proposed. After the calculated value of depth of peak penetration resistance, $d_{\text{peak\_cal}}$, is introduced into the model factor ε_{d}, the relationship between the measured value, $d_{\text{peak\_mea}}$, and the calculated value can be expressed as (Li *et al.*, 2018):

$$d_{\text{peak\_mea}} = d_{\text{peak\_cal}} \times \varepsilon_{\text{d}} \tag{4}$$

A similar analysis is performed on the peak penetration resistance (Li *et al.*, 2018):

$$q_{\text{peak\_mea}} = q_{\text{peak\_cal}} \times \varepsilon_{\text{q}} \tag{5}$$

where $q_{\text{peak\_mea}}$ is the measured value of peak penetration resistance; $q_{\text{peak\_cal}}$ is the calculated value of peak penetration resistance; and ε_{q} is the model factor.

The data sets are processed to obtain calculated values $d_{\text{peak\_cal}}$, $q_{\text{peak\_semi}}$ and $q_{\text{peak\_pro}}$ (as shown in Figure 2). They are combined with the measured value $d_{\text{peak\_mea}}$ and $q_{\text{peak\_mea}}$, and the model factors ε_{d}, $\varepsilon_{\text{q\_semi}}$ and $\varepsilon_{\text{q\_pro}}$ are obtained according to Eqs. (4) and (5). The calculated values of peak penetration resistance and the corresponding depth are quite different from the measured values, as shown in Figure 2. The model factors have great discreteness and their frequency histograms are shown in Figure 3. It can be seen that the model factors need to be described by probability distribution. Beta distribution has strong flexibility and applicability, and changing the shape parameters of its density function can change the Beta distribution from uniform distribution to approximate normal distribution. Therefore, the model factors are assumed to be Beta distribution. The probability density function is expressed as (He, 1991):

$$f\left(x,\gamma,\eta,a,b\right)=\begin{cases}\dfrac{1}{(b-a)B(\gamma,\eta)}\left(\dfrac{x-a}{b-a}\right)^{\gamma-1}\left(1-\dfrac{x-a}{b-a}\right)^{\eta-1}, a\le x\le b\\ 0\end{cases} \tag{6}$$

where $B(\gamma,\eta)=\int_0^1 z^{\gamma-1}(1-z)^{\eta-1}dz,(\gamma,\eta>0),z=(x-a)/(b-a)$, γ and η are the shape parameters, a and b are lower and upper limits of the distribution.

The shape parameters of the Beta distribution are shown in Table 1, and the fitting curves are shown in Figure 3. The peak penetration resistance and the corresponding depth prediction range obtained by the model factors are shown in the yellow area in Figure 4. The measured values of peak penetration resistance and the corresponding depth are included in the range of possible values obtained by the Beta distribution.

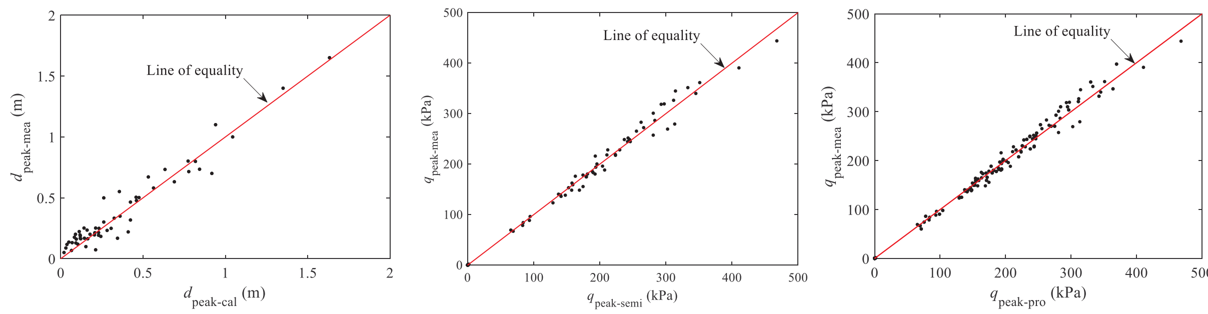

(a) (b) (c)

Figure 2. Relationship between calculated values and measured values: (a) the depth of peak penetration resistance, (b) the semi-empirical peak penetration resistance and (c) the improved ISO calculation of peak penetration resistance

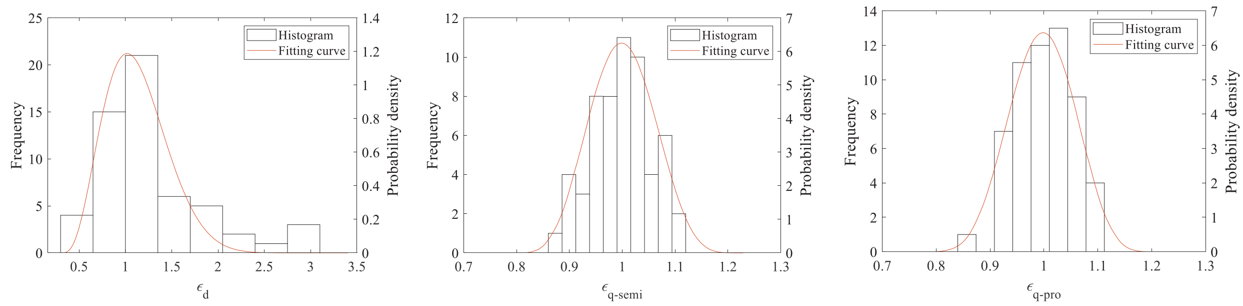

(a) (b) (c)

Figure 3. Frequency histogram and Beta fitting of model factor:(a) the model factor of the depth, (b) the model factor of the semi-empirical equation and (c) the model factor of improved ISO equation

Table 1. Shape parameters of Beta fitting

Model factor		Shape parameters	
		γ	η
Depth	ε_{d}	4.16	11.62
Stress	ε_{q_semi}	5.90	6.43
	ε_{q_pro}	7.05	6.09

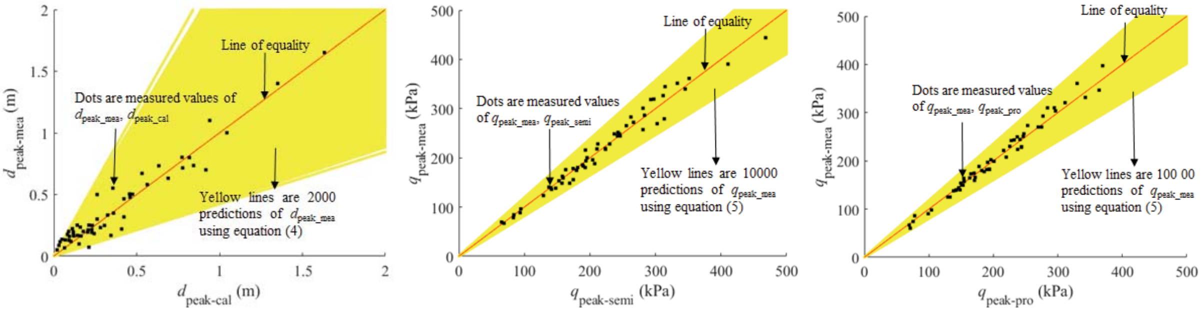

(a) (b) (c)

Figure 4. Relationship between measured value and predicted range value of probability model: (a) the depth of peak penetration resistance, (b) predicted range value of the semi-empirical model and (c) predicted range value of the improved ISO model

3.2 Bayesian estimation of punch-through probability

The candidate values of the peak penetration resistance and the corresponding depth during spudcan penetration are set as q_{pi}, d_{pj} (i, j = 1,2,3...), respectively. Assuming that the peak penetration resistance and the corresponding depth are independent of each other, the prior probability P (q_{pi}, d_{pj}) is the product of P (q_{pi}) and P (d_{pj}), where P (q_{pi}) is marginal probability of peak resistance occurring at the ith candidate stress, and P (d_{pj}) is marginal probability of peak resistance occurring at the jth candidate depth. The Bayesian equation is used to update the punch-through prediction, which can be expressed as (Marco *et al*., 2017; Li *et al*., 2018):

$$P(q_{pi}, d_{pj} \mid q_{mon}, d_{mon}) = \frac{P(q_{pi}, d_{pj}) \cdot P(q_{mon}, d_{mon} \mid q_{pi}, d_{pj})}{\sum_{i,j} P(q_{pi}, d_{pj}) \cdot P(q_{mon}, d_{mon} \mid q_{pi}, d_{pj})} \tag{7}$$

where q_{mon} is the monitored penetration resistance; d_{mon} is the monitored penetration depth; P (q_{mon}, d_{mon} | q_{pi}, d_{pj}) is the likelihood; and P (q_{pi}, d_{pj} | q_{mon}, d_{mon}) is the posterior probability.

3.2.1 Prior probability

Take N random numbers subject to Beta distribution respectively to obtain ε_q and ε_d, and substitute them into Eqs. (4) and (5) to obtain measured value q_{peak_mea} and d_{peak_mea}. The measured value q_{peak_mea} is equally divided into (N_m-1) segments, and the length of each segment is Δ. Then take these d_{peak_mea} as the center point of Δ, and the frequency of Δ is taken as the marginal probability P (d_{pj}) (i = 1,2,3,..., N_m). A similar analysis is performed on the peak penetration resistance. The calculation of a prior probability is expressed as (Marco *et al*., 2017; Li *et al*., 2018):

$$P(q_{pi}, d_{pj}) = P(q_{pi}) \cdot P(d_{pj}) \tag{8}$$

3.2.2 Likelihood and posterior probability

The likelihood P (q_{mon}, d_{mon} | q_{pi}, d_{pj}) represents the probability that the monitored data is (q_{mon}, d_{mon}) when the punch-through failure occurs at the predicted candidate value (q_{pi}, d_{pj}). Hossain and Randolph (2009b) proposed the logarithmic relationship between the ratio q_{mon} / q_{peak} and the ratio d_{mon} / d_{peak}. On this basis, Marco *et al*. (2017) proposed a normalized load-displacement probability model, which is also used to calculate the likelihood in this study.

$$d_{pred} = d_{pj} \times \left(\frac{q_{mon}}{q_{pi}} \right)^{\frac{1}{\eta_b}} \tag{9}$$

$$\eta_b = 0.154 \times \chi^{0.515} + \varepsilon_b \tag{10}$$

$$\chi = \frac{S_{ubs}}{S_{ut}} \times \frac{t}{D} \times (1 + \frac{kD}{S_{ubs}}) \tag{11}$$

where d_{pred} is the predicted value of penetration depth when the monitoring value of penetration resistance is q_{mon}; η_b is the load-displacement model factor; and χ is versus the auxiliary parameter.

Once prior probabilities and likelihood values are available for all punch-through resistance and the corresponding depth, the posterior probability is calculated from Bayesian equation.

4 Illustrative Examples

The centrifuge test E2UU-IV-T11 of Hossain and Randolph (2010a) is analyzed by the Bayesian prediction method. Detailed in Table 2 are the geometric and soil properties tested (γ_t' and γ_b' are the effective unit weight of top-layer soil and bottom-layer soil respectively). In this example, the peak penetration resistance is 324 kPa occurring at 1.30 m. The peak penetration resistance calculated by semi-empirical model and improved ISO model are 292 kPa and 310 kPa, and the calculated value of the corresponding depth is 1.69 m. The peak penetration depth is much smaller than that calculated from the deterministic model, which may pose threat to the structures.

Table 2. Summary of centrifuge test

Specimen	Group	Test	D (m)	T (m)	t/D	γ_t' (kN/m3)	γ_b' (kN/m3)	Sut (kPa)	Subs (kPa)	k (kPa/m)
Event2	IV	T11	6	7.5	1.25	8.13	7.75	47.3	14	0

Generate 2000000 random numbers about ε_q and ε_d respectively. These random numbers, q_{peak_cal} and d_{peak_cal} are substituted into Eqs. (4) and (5). Then, q_{peak_mea} and d_{peak_mea} are divided equally into 50 segments to obtain q_{pi} and d_{pj} (i, j = 1,2,3..., 51). The interval length Δ of each segment is calculated, and the q_{pi} and d_{pj} are taken as the midpoint of Δ. The frequency of each segment Δ is taken as the marginal probability P (q_{pi}) and P (d_{pj}) respectively. Therefore, the prior probability P (q_{pi}, d_{pj}) is a 51 × 51 matrix and the prior probability contours can be obtained by connecting the points with equal prior probability values. Figure 5 is the prior probability obtained by the semi-empirical model and the improved ISO model. No matter which deterministic model is adopted, the calculated value is very different from the measured value. The prior probability for the measured values are 0 and 0.003 respectively, as shown in Figure 5. It should be noted that the exact probability values of the peak behavior for any specific couple of candidate values (q_{pi}, d_{pj}) are a function of the user-defined number of discretization.

The monitoring data of spudcan in the process of penetration are shown in Table 3. The likelihood is calculated by the load-displacement model (Marco *et al.* 2017). Then, the posterior probability is obtained according to Eq. (7). Figure 6 (a) and (b) (Figure 8 (a) and (b)) are the likelihood for one and five sets of monitoring data respectively. For example, the red hollow circle shown in Figure 6 (a) represents the monitoring data. If the spudcan occurs punch-through at a candidate value (q_{pi}, d_{pj}), the probability value is the likelihood when the monitoring data is (277 kPa, 0.12 m) during spudcan penetration.

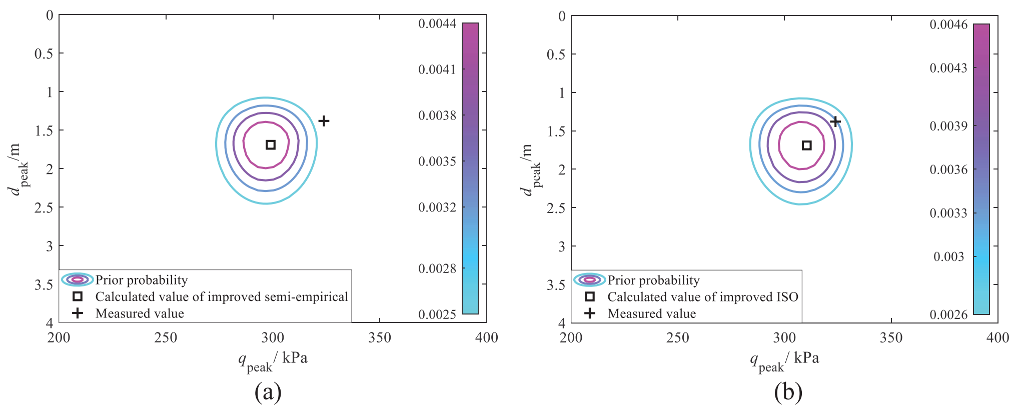

Figure 5. Prior probability contours obtained by: (a) the semi-empirical model and (b) the improved ISO model

Table 3. Monitoring data

Number of monitoring data	q_{mon} (kPa)	d_{mon} (m)
1	277	0.12
2	291	0.36
3	303	0.66
4	313	0.84
5	320	1.08

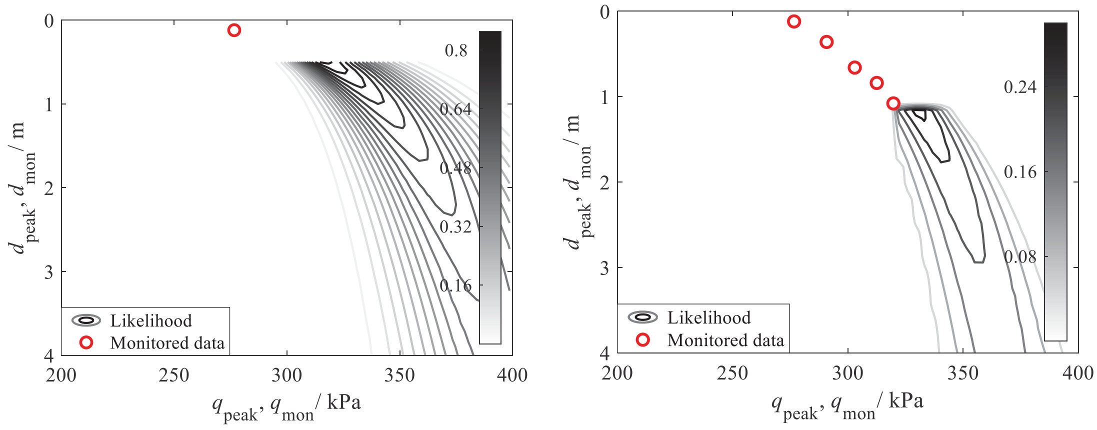

(a) (b)

Figure 6. Likelihood of the semi-empirical model: (a) 1 observation and (b) 5 observations

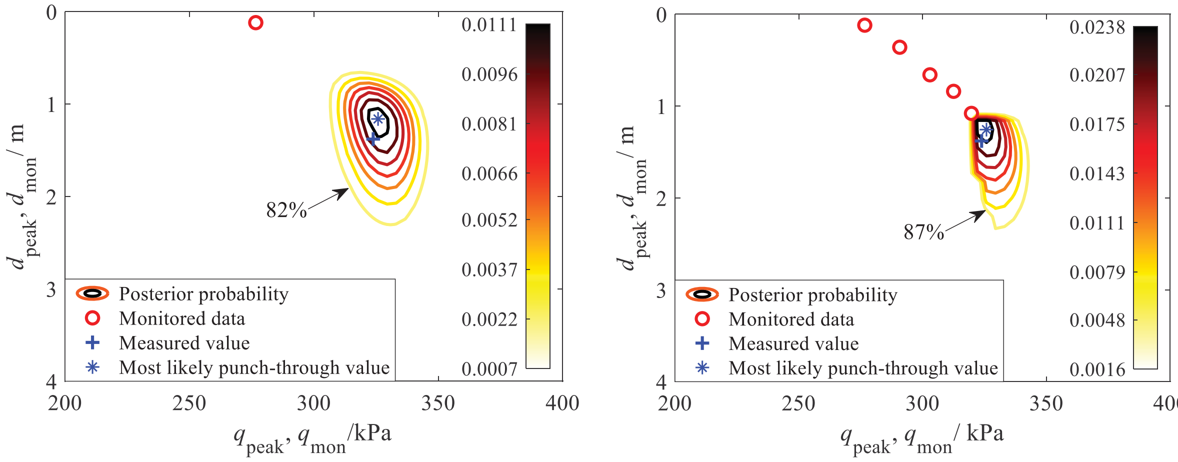

(a) (b)

Figure 7. Posterior probabilities of the semi-empirical model: (a) 1 observation and (b) 5 observations

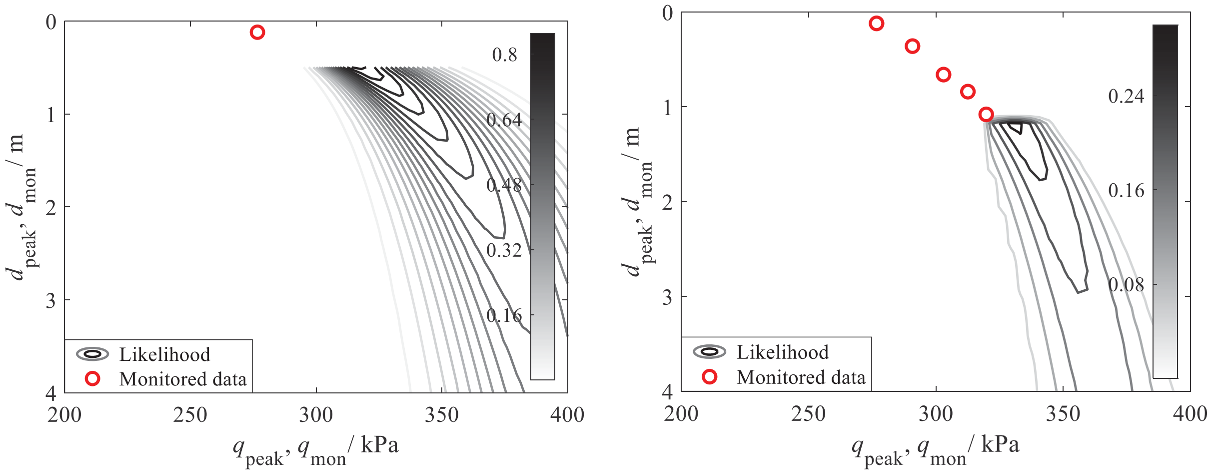

(a) (b)

Figure 8. Likelihood of the improved ISO model: (a) 1 observation and (b) 5 observations

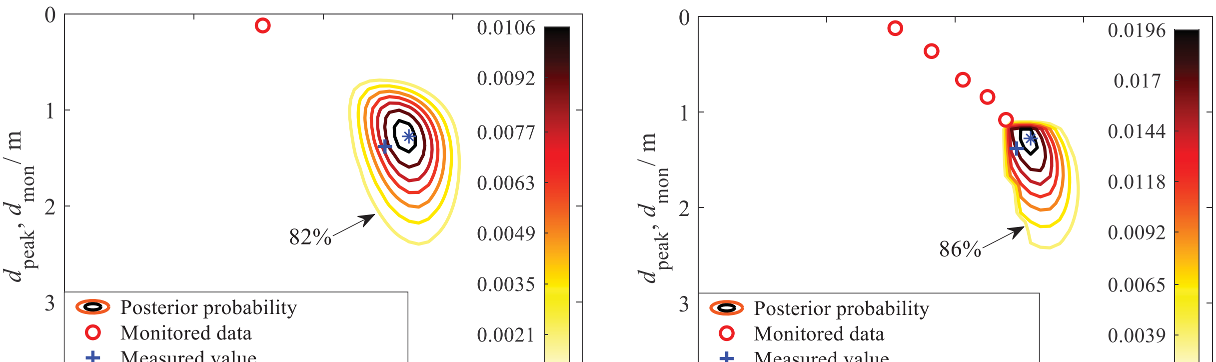

Figure 7 (a) and (b) (Figure 9 (a) and (b)) are the posterior probability of peak penetration resistance and the corresponding depth for one and five sets of monitoring data respectively. Contour plots allow intuitive visualization of the data, with the quoted percentages representing the probability that the peak penetration resistance and the corresponding depth will lie within the contour. For example, there is 82% probability in Figure 7 (a) that the peak values lie within the first contour where the peak penetration resistance is from 308 kPa to 347 kPa, and the corresponding depth is from 0.69 m to 2.30 m. As the number of monitoring data increases, the more concentrated the area surrounded by contour lines and the greater the updated the posterior probability shown in Figure 7(b) (i.e. the range within which there is 87% chance that the peak resistance lies within is only from 319 kPa to 344 kPa, and depth from 1.07 m to 2.30 m). The "*" in Figure 7 (a) and (b) (Figure 9 (a) and (b)) indicates failure most likely to occur at this point within the predicted punch-through area. With the increase of monitoring data, the point is closer and closer to the measured value. The coordinate of this point is (326 kPa, 1.26 m) in Figure 7 (b) and the relative error between it and the measured value (324 kPa, 1.30 m) is 1% in peak penetration resistance and 3% in depth. The coordinate of this point is (329 kPa, 1.27 m) in Figure 9 (b) and the relative error between it and the measured value is 2% in peak penetration resistance and 2% in depth. There is little difference between the predicted results.

This example has demonstrated that the areas where punch-through may occur is constantly updated with the increase in monitoring data. Furthermore, the punch-through area is more and more concentrated, and the posterior probability at the measured value is also greater. No matter which deterministic model of peak resistance is used, the results obtained by the Bayesian method can well predict punch-through.

5 Conclusions

This paper develops Bayesian prediction model, and two deterministic models of peak penetration resistance are used in Bayesian method to predict the punch-through failure of spudcan in stiff-over-soft clays. Whether the deterministic model adopts semi-empirical model or improved ISO model, the predicted punch-through area is almost consistent with its corresponding posterior probability, and the difference between the predicted peak values at the most likely punch-through point and the measured value is within 5%. Moreover, compared with the deterministic analysis method to predict the punch-through, the results obtained by the probability method can be updated in real time, and the updated prediction results are closer to the measurements. The Bayesian prediction method has good robustness. It provides operation instructions for technicians during the installation of spudcan foundation.

Acknowledgements

This work was supported by the Natural Science Foundation of China [grant number 51979067].

References

Brown, J.D., and Meyerhof, G.G. (1969). Experimental study of bearing capacity in layered clays. *In Proceedings of the 7th International Conference on Soil Mechanics and Foundation Engineering, Mexico*, 2, 45–51.

He, J.R. (1991). Estimating the distributions of manufactured dimensions with the beta probability density function. *Mach. Tools Manufact*, 31(3), 383-396.

Hossain, M.S., and Randolph, M.F. (2009). New mechanism-based design approach for spudcan foundations on stiff-over-soft clay. *In Proceedings of the Offshore Technology Conference, Houston*, OTC 19907.

Hossain, M.S., and Randolph, M.F. (2010). Deep-penetrating spudcan foundations on layered clays: centrifuge tests. *Géotechnique*, 60(3), 157–170.

Hu, P., Stanier, S. A., Cassidy, M. J. and Wang, D. (2014). Predicting peak resistance of spudcan penetrating sand overlying clay. *Journal of Geotechnical and Geoenvironmental Engineering*, 140(2), 04013009.

ISO (International Organization for Standardization). (2016). ISO/FDIS 19905-1: Petroleum and natural gas industries – Site-specific assessment of mobile offshore unit – Part 1: Jack-ups. *Geneva, Switzerland: ISO*.

Jack, R. L., Hoyle, M. J. R., Smith, N. P. & Hunt, R. J. (2013). Jack-up accident statistics – a further update. *Proceedings of the 14th international conference on the jack-up platform design, construction and operation, London, UK*.

Li, J. H., Hu, P., Uzielli, M. and Cassidy, M. J. (2018). Bayesian prediction of peak resistance of a spudcan penetrating sand-over-clay. *Géotechnique*, 68(10), 905-917.

Marco Uzielli, Mark J. Cassidy, Muhammad S. Hossain. (2017). Bayesian Prediction of Punch-Through Probability for Spudcans in Stiff-over-Soft Clay. *Geotechnical Safety and Reliability*, 286, 247-265.

Menzies, D., and Lopez, C.R. (2011). Four atypical jack-up rig foundation case histories. *In Proceedings of the 13th International Conference on the Jack-up Platform: Design, Construction and Operation, London*.

Osborne, J. J. and Paisley, J. M. (2016). SE Asia jack-up punch throughs: The way forward? In Offshore site investigation and geotechnics – sustainability and diversity, London, UK: *Society for Underwater Technology*, 301–306.

SNAME (2008). Recommended practice for site specific assessment of mobile jack-up units. T&R Bullitin 5-5 and 5- 5A, 3st Edition-Rev.3, *Society of Naval Architects and Marine Engineers, Alexandria*.

Van Dijk, B. F. J. and Yetginer, A. G. (2015). Findings of the ISSMGE jack-up leg penetration prediction event. *In Frontiers in offshore geotechnics III (ed. V. Meyer), Boca Raton, FL, USA: CRC Press*, 1267–1274.

Zheng, J., M.S. Hossain, and D. Wang. (2016). Prediction of spudcan penetration resistance profile in stiff-over-soft clays, *Canadian Geotechnical Journal*, 53(12), 1978–1990.